Fate and transport of metals in H_2S-rich waters at a treatment wetland

Christopher H. Gammons[a] and Angela K. Frandsen[b]†

[a] *Montana Tech of the University of Montana, Department of Geological Engineering, Butte, Montana, 59701. E-mail: cgammons@mtech.edu*
[b] *Montana Tech of the University of Montana, Department of Environmental Engineering, Butte, Montana, 59701*

Article

Received 12th October 2000, Accepted 26th January 2001
Published on the Web 8th February 2001

The aqueous geochemistry of Zn, Cu, Cd, Fe, Mn and As is discussed within the context of an anaerobic treatment wetland in Butte, Montana. The water being treated had a circum-neutral pH with high concentrations of trace metals and sulfate. Reducing conditions in the wetland substrate promoted bacterial sulfate reduction (BSR) and precipitation of dissolved metal as sulfide minerals. ZnS was the most common sulfide phase found, and consisted of framboidal clusters of individual spheres with diameters in the submicron range. Some of the ZnS particles passed through the subsurface flow, anaerobic cells in suspended form. The concentration of "dissolved" trace metals (passing through a 0.45 μm filter) was monitored as a function of H_2S concentration, and compared to predicted solubilities based on experimental studies of aqueous metal complexation with dissolved sulfide. Whereas the theoretical predictions produce "U-shaped" solubility curves as a function of H_2S, the field data show a flat dependence of metal concentration on H_2S. Observed metal concentrations for Zn, Cu and Cd were greater than the predicted values, particularly at low H_2S concentration, whereas Mn and As were undersaturated with their respective metal sulfides. Results from this study show that water treatment facilities employing BSR have the potential to mobilize arsenic out of mineral substrates at levels that may exceed regulatory criteria. Dissolved iron was close to equilibrium saturation with amorphous FeS at the higher range of sulfide concentrations observed (>0.1 mmol H_2S), but was more likely constrained by goethite at lower H_2S levels. Inconsistencies between our field results and theoretical predictions may be due to several problems, including: (i) a lack of understanding of the form, valence, and thermodynamic stability of poorly crystalline metal sulfide precipitates; (ii) the possible influence of metal sulfide colloids imparting an erroneously high "dissolved" metal concentration; (iii) inaccurate or incomplete thermodynamic data for aqueous metal complexes at the conditions of the treatment facility; and (iv) difficulties in accurately measuring low concentrations of dissolved sulfide in the field.

1. Introduction

The purpose of this paper is to critically examine the geochemical behavior of trace metals in an engineered, H_2S-rich treatment wetland. In the past decade, constructed wetlands and/or reactive barriers that employ bacterial sulfate reduction have emerged as one of the more promising passive treatment technologies for the remediation of metal-impacted waters.[1–8] The design of such facilities relies on subsurface flow of water and maintenance of permeable, anaerobic conditions. Reducing conditions are generated by amending the substrate with organic carbon, usually in the form of manure or compost. Sulfate reducing bacteria (*Desulfovibrio sp.*) catalyze the reduction of dissolved sulfate in the polluted water to hydrogen sulfide, and metals are immobilized as sulfide minerals, as shown by the following reactions:

$$SO_4^{2-} + 2CH_2O\,(org) \Rightarrow H_2S + 2HCO_3^- \quad (1)$$

$$H_2S + Me^{2+} = MeS(s) + 2H^+ \quad (2)$$

where Me = any divalent metal cation. Although reaction (1) produces 2 moles of bicarbonate alkalinity, the acidity produced by reaction (2) tends to offset this, such that protons are conserved in the overall reaction:

$$SO_4^{2-} + Me^{2+} + 2CH_2O(org) = MeS(s) + 2H_2CO_3(aq) \quad (3)$$

However, in a treatment wetland or SRB bioreactor, it is often the case that more H_2S is generated *via* reaction (1) than is consumed *via* precipitation of sulfide minerals. Such systems see a net increase in alkalinity, and often produce considerable quantities of excess H_2S.[9] The possible adverse affects of excess H_2S have not received much attention in the engineering literature to date. Besides being a highly toxic substance, H_2S is known to form stable aqueous compounds with many heavy metals. A good example is cadmium, for which the following general solubility reaction may be written:

$$CdS(s) + (n \quad 1)H_2S = Cd(HS)_n^{2\ n} + (n \quad 2)H^+ \quad (4)$$

Fig. 1 shows the calculated solubility of amorphous CdS as a function of H_2S concentration, based on equilibrium constants from Wang and Tessier[10] for reaction (4), where $n = 0$ to 4. The "U-shaped" solubility dependence for CdS is very similar to the amphoteric relationship between metal oxide solubility and pH, which is much more familiar to water treatment engineers. Just as there is an optimal pH range for maximum metal removal during lime treatment of mining-impacted waters, there is an optimal H_2S concentration for metal removal *via* sulfide treatment. Increases in H_2S above this

†Present address: CDM Federal Programs Corporation, Helena, Montana 59601. E-mail: frandsenak@cdm.com

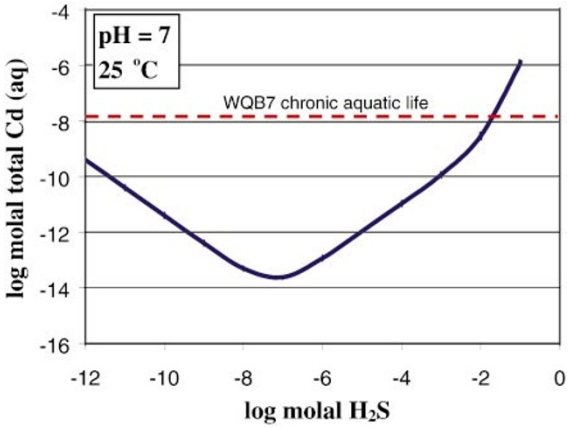

Fig. 1 The solubility of amorphous CdS as a function of H_2S concentration at pH = 7, 25 °C (solubility curve calculated from Wang and Tessier[10]). Also shown is the Montana aquatic life standard for chronic exposure to cadmium, indexed to 100 mg L^{-1} $CaCO_3$ alkalinity.

optimal level could theoretically result in enhanced metal solubility, compromising the performance of the treatment facility.

The behavior of iron and trace metals in low temperature H_2S-rich waters has been extensively studied in natural environments, such as anoxic seawater,[11] marine sediments,[12,13] salt marshes and estuaries,[14,15] and fresh water lakes.[16–19] Although constructed wetlands are analogous in many respects to natural H_2S-rich systems, they differ from the point of view that the waters being treated often have much higher metal concentrations. This is certainly true for the Wetlands Demonstration Project 1 (WDP1) site in Butte, Montana, which is the focus of this study. Although built as a treatment facility, data from WDP1 provide insight into the chemical, physical, and biological processes which interplay in low temperature, sulfidic waters. The closest natural analog to the WDP1 facility would be a wetland in a temperate climate that receives loadings of metals and sulfate, either due to anthropogenic impacts (*e.g.*, acidic mine drainage), or as a natural consequence of weathering of sulfide-rich ore bodies. Such wetland systems are rare, but have been documented in the literature.[20–23] The results of this study are also directly applicable to other treatment operations employing H_2S, such as constructed wetlands, bioreactors, or reactive barriers.

2. Methods

2.1 Wetlands Demonstration Project 1

The Wetlands Demonstration Project 1 (WDP1) facility was built by the Atlantic Richfield Company (ARCO) to test the feasibility of using anaerobic wetlands as a passive treatment scheme for contaminated water in the Metro Storm Drain (MSD). The MSD is a diversion ditch located at the bottom of Butte Hill, which intercepts shallow groundwater and surface runoff generated during storms and snow melt. Soils, groundwater and surface water in the area are highly contaminated with metals—a legacy of over 100 years of mining, milling, and smelting of polymetallic mineral deposits in the Butte district.[24,25] Although an unimpressive body of water (Fig. 2), the MSD is in fact the headwaters of the Clark Fork River of the Columbia River drainage, and is part of the largest contiguous superfund site in the United States. The MSD has a near-neutral pH (6.0 to 7.0), but contains concentrations of heavy metals far above regulatory standards.

WDP1 operated continuously for 3 years, from May 1996 through December 1998. The facility consisted of seven treatment cells with different dimensions and substrate

Fig. 2 Photograph of Butte's Metro Storm Drain, taken in November 1997. Note the high turbidity (despite low flow and no precipitation for several weeks), due to abundance of suspended iron oxy-hydroxide particles.

compositions (Fig. 3, Table 1). MSD water was first pumped into a surge pond (Cell 0), which allowed settling of suspended particles, and provided hydraulic head and water storage for the rest of the facility. Water exiting the surge pond passed by gravity through one of four parallel, subsurface-flow, anaerobic cells (cells 1, 2, 3, 4). The main purpose of the anaerobic cells was to provide a suitable environment for sulfate-reducing bacteria (SRB), with subsequent precipitation of heavy metals as insoluble sulfide minerals. The anaerobic cells were lined on the bottom with HDPE, were filled with *ca.* 0.5 inch river gravel and limestone fragments, and (with the exception of cell 3) were

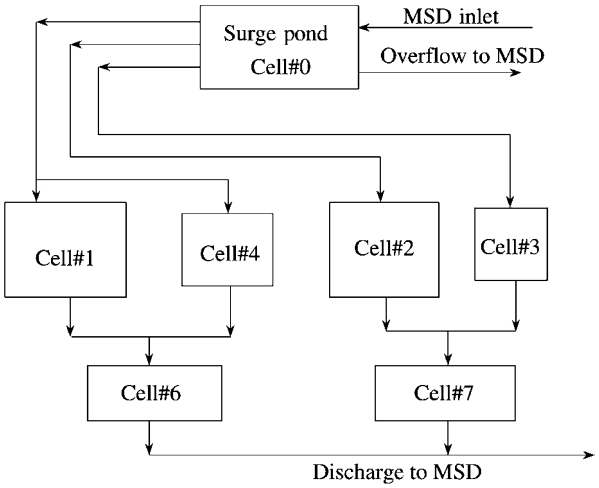

Fig. 3 Schematic diagram of the Wetlands demonstration project 1 (not to scale). See Table 1 for further specifications.

Table 1 Description of wetland cells at WDP1

Cell	Description	Specifications	HRT[a] and design flow
0	Settling pond	Area = 7000 ft^2 (1 foot = 0.3048 m), volume = 40 000 ft^3	10 days and 20 gpm[b]
1	Anaerobic wetlands	Horizontal subsurface flow volume = 30 000 ft^3, depth = 2.5 ft 100% river gravel + limestone fragments	9.4 days and 5 gpm
2	Anaerobic wetlands	Horizontal subsurface flow volume = 20 000 ft^3, depth = 4 ft 80% river gravel + limestone, 20% compost	6.2 days and 5 gpm
3	Anaerobic wetlands	Upwards subsurface flow volume = 12 000 ft^3, depth = 6 ft 50% river gravel + limestone, 50% compost	3.7 days and 5 gpm
4	Anaerobic wetlands	Horizontal subsurface flow volume = 15 000 ft^3, depth = 2.5 ft 100% river gravel + limestone fragments	4.8 days and 5 gpm
6	Aerobic wetlands	Shallow ponds and riffles area *ca.* 2000 ft^2	*Ca.* 2 days and 10 gpm
7	Aerobic wetlands	As for cell 6, area *ca.* 6500 ft^2	*Ca.* 6 days and 10 gpm

[a]HRT = hydraulic residence time. [b]gpm = gallons per minute (1 gallon = 4.54609 dm^3).

planted at the surface with cattails (*Typha latifolia*) as a renewable source of organic carbon. A composted mixture of sewage sludge and wood chips was added to the substrates of cells 2 and 3 to further encourage SRB growth. Water exiting the anaerobic cells flowed into one of two aerobic polishing cells (cells 6 and 7), which consisted of a series of shallow pools and riffles. The purpose of these cells was to re-aerate the water, oxidize any excess H_2S, and hopefully remove residual iron and manganese as oxy-hydroxide phases. The entire WDP1 facility treated between 15 and 30 gpm of MSD water during the 3 years of operation.

2.2 Water chemistry monitoring

Between 1996 and 1998, the water chemistry of WDP1 was monitored closely by Montana Tech staff and students, and was recorded in an Access database. Each month, water samples were taken at sampling stations near the outlet to each of the seven cells for filtered metals, total metals, anions, dissolved sulfide, and total/organic carbon. Monthly environmental parameters (temperature, pH, Eh, SC, dissolved oxygen, alkalinity) were also collected at each sampling station. In addition to the effluent samples, each of the anaerobic cells contained a network of internal piezometers. These piezometers were used to monitor the distribution of chemical gradients inside the cell as a function of depth and distance from the inlet. The internal piezometers were sampled approximately 3–4 times per year, with the exception of cell 3, for which internal sampling was discontinued after the first year of operation. Each piezometer was equipped with its own dedicated teflon tubing assembly, which included a 1–3 ft long teflon plug to prevent freezing in winter. Sampling and collection of environmental parameters were accomplished using a peristaltic pump and a low volume flow cell.

All metal samples were acidified to 2% HCl or HNO_3 using Fisher Trace Metal Grade acid, and were refrigerated prior to analysis. The samples were analyzed for the elements As, Al, Ca, Cd, Cr, Co, Cu, Fe, S, P, Pb, Ni, K, Mg, Mn, Na, Si, and Zn, using a Perkin Elmer Optima 3000 DV ICP-AES spectrometer. Analytical protocol for this instrument followed SW-846 method 6010B, inorganic analysis by ICP-AES and EPA 600 method 200.7, inorganic analysis by inductively coupled plasma analysis. Filtration was performed in the field using disposable 0.45 μm CAMEO 25GA acetate-plus membrane syringe filters with 1 μm glass prefilters. The inorganic anions fluoride, chloride, nitrite, bromide, nitrate, orthophosphate, and sulfate were determined using a Dionex System DX-500 ion chromatograph, following EPA Method 300.0. Dissolved sulfide was determined using the Methylene Blue method (HACH method 8131), and a HACH DR-2010 portable spectrometer. Samples collected for sulfide analysis were obtained directly with a syringe from the low volume flow cell during pumping. The samples were stabilized in the field by filtration to 0.22 μm and immediate transfer to disposable cuvettes containing the methylene blue reagent. Duplicate sampling indicated minimal loss of H_2S occurred due to volatilization or oxidation during sampling and prior to analysis.

During the last year of operation, each internal piezometer in cells 1, 2 and 4 was equipped with a small cup near the base of the sampling tube. These cups collected solid particles that passed through the piezometer screens during pumping. The cups were sampled in November 1998, and the solids were stored in tightly sealed glass vials filled completely with original site water, and placed in a refrigerator. The solids were examined periodically in 1999 and early 2000 by SEM and XRD, using equipment in the Department of Metallurgical Engineering, Montana Tech, and the Instrumental and Chemical Analysis Laboratory (ICAL), Montana State University.

3. Results

Because the WDP1 database includes such a vast amount of data, only selected results relevant to this paper are reported and discussed here. An Excel spreadsheet is available upon request from the senior author which summarizes all WDP1 data entries for which dissolved sulfide is available, as well as the sample location, date, temperature, pH, and results for selected filtered and unfiltered metals (As, Cu, Cd, Fe, Mn, Zn). This spreadsheet was the database on which all of the calculations in the Discussion section of this paper were based.

Before discussing each metal–sulfide system in detail, a brief summary of seasonal changes in selected water quality parameters at WDP1 is presented. Aspects of the overall performance of the WDP1 facility have been summarized elsewhere.[9,26–30] Additional details may be found in Montana Tech MSc theses.[31–37]

3.1 Environmental parameters

Table 2 lists selected chemical parameters for the influent and effluent waters to cell 2 (horizontal, subsurface-flow anaerobic cell, with compost), for a typical winter and summer sampling event. Butte is relatively dry (*ca.* 12 in of precipitation per year), but experiences extremes in temperature. Water temperature at the site varied from a low of near freezing in mid-winter, to a high of *ca.* 20 °C in August. The pH of influent waters ranged from 6.0 to 7.0, with a 3-year mean of 6.78. No consistent trend in pH was noted with the seasons. The pH of water passing through cell 2 typically showed no change, or increased slightly (*e.g.*, 0.1 to 0.3 log units). Much more significant increases in alkalinity, total inorganic carbon, and H_2S, and decreases in Eh and sulfate, were observed as water passed through cell 2 (Table 2). These changes were all augmented in the summer, and are mainly attributed to increases in the rate of bacterial sulfate reduction (BSR).

Based on the observed decreases in dissolved sulfate

Table 2 Concentration of selected parameters in cell 2. (Modified from Table 2 of Gammons *et al.*[9])[a]

	Summer (8/17/98)			Winter (2/19/98)		
Parameter	Influent	Effluent	Removal efficiency	Influent	Effluent	Removal efficiency
T/°C	19.0	19.1		2.0	2.7	
pH	6.80	6.84		6.42	6.73	
SC/μS cm^{-1}	872	1070		821	897	
Alkalinity	66.3	178		72	149	
DIC[b]/mg C L^{-1}	16.1	54.4		18.3	36.4	
Eh/mV	476	−153		493	76	
As	8.6	11.9	(−38%)	7.3	5.2	28.8%
Cd	40.5	0.51	98.7%	32.7	0.52	98.4%
Cu	123	3.6	97.0%	216	1.0	99.5%
Fe	28.8	18.0	37.5%	171	528	(−209%)
Mn	6680	3640	45.5%	7070	8080	(−14%)
Zn (filtered)	9330	10.5	99.9%	9950	101	99.0%
Zn (unfiltered)	9850	42.9	99.6%	10,000	640	93.6%
Sulfate/mg SO_4 L^{-1}	472	289	38.8%	336	313	6.8%
H_2S/mg H_2S L^{-1}	0.0	34.1		0.0	2.0	

[a]Heavy metals = μg L^{-1}, filtered (0.45 μm); alkalinity = mg $CaCO_3$ L^{-1}. [b]DIC = dissolved inorganic carbon.

concentration, Gammons *et al.*[9] estimated a maximum mid-summer BSR rate of *ca.* 0.4 millimoles of H_2S produced per liter of water per day. Of the total H_2S produced, a significant percentage was immobilized as sulfide minerals, an unknown fraction was volatilized to the air, and the remainder exited the cells in dissolved form, or as colloidal particles of elemental sulfur. Machemer *et al.*[1] conducted a more detailed S mass balance for a similar treatment wetland in Colorado, and concluded that loss of H_2S due to volatilization was minor (<1% of the total sulfide generated). Nonetheless, the WDP1 facility did smell foul most of the year, indicating potentially significant H_2S discharges to the atmosphere.

Dissolved sulfide concentrations of cell 2 effluent waters were typically >1 mg L^{-1}, sometimes as high as 30 mg L^{-1}. In the winter months, BSR rates and effluent H_2S concentrations were approximately ten times lower than in summer, and most of the observed increases in alkalinity and DIC in winter have been attributed to dissolution of limestone in the substrate.[9] In cells 6 and 7, excess H_2S leaving the anaerobic cells in dissolved form was incompletely oxidized to elemental sulfur by a combination of white and purple bacteria (Fig. 4). This phenomenon caused water in the down-gradient aerobic polishing ponds to take on the appearance of dilute skim milk (Fig. 5).

Fig. 4 Photograph of purple and white S-oxidizing bacteria near the outlet distribution pipe for cells 2 and 3. The purple bacteria are incompletely oxidizing H_2S to elemental sulfur. Similar growths of purple bacteria have been reported for H_2S-rich effluent waters at other constructed wetlands (James Gusek, personal communication, 1999). Although bacterial identification was not attempted in this study, it is likely[78] that the purple microbes include the *Chromatiaceae* and possibly *Rhodospirillaceae*, whereas an anonymous reviewer of this article suggested the filamentous white bacteria could be *Beggiatoacea*.

3.2 Metal attenuation

The main metals of concern at WDP1 were copper, cadmium, zinc and manganese. Iron and arsenic are also discussed here, although dissolved concentrations of these metals entering WDP1 were low. Table 2 summarizes removal efficiencies for these metals in cell 2 for a typical summer and winter sampling event.

Removal of Cd and Cu was excellent year-round in all of the anaerobic cells. The most likely attenuation mechanism was

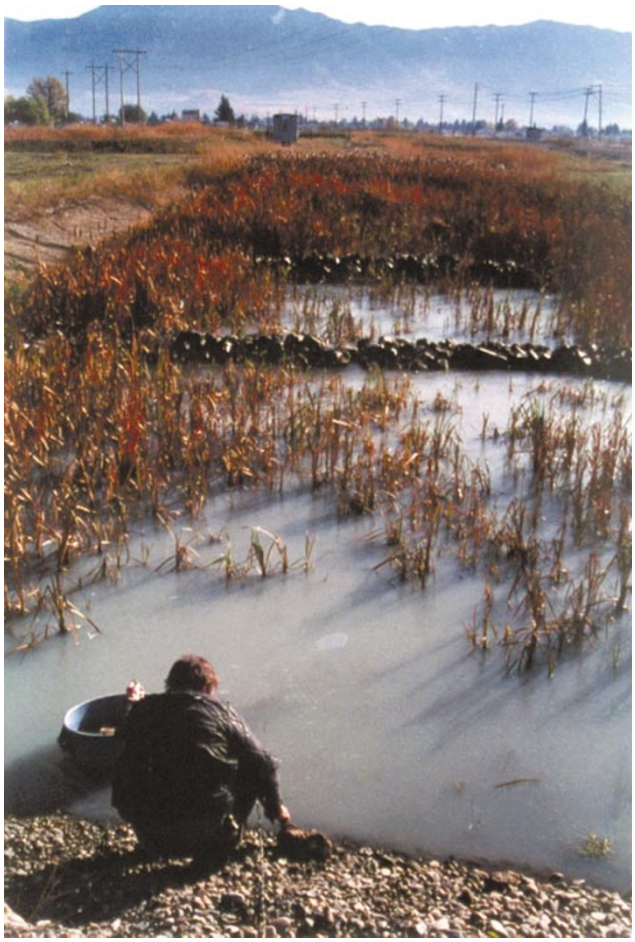

Fig. 5 Photograph of the aerobic polishing pond cell 7, looking upgradient from the outlet. Photo taken in November 1997. Note the turbid, milky white color imparted by suspended particles of elemental sulfur.

precipitation of insoluble sulfide minerals. Sulfide minerals of cadmium and copper have exceedingly low solubility products;[38] consequently, these metals would have been immediately scavenged by H_2S as it was formed by BSR. Geochemical modeling indicates that cadmium could also have been attenuated as impurities in calcite (*i.e.*, $CdCO_3$–$CaCO_3$ solid solution). There is a strong thermodynamic driving force for cadmium to be scavenged to very low levels by carbonate minerals.[39,40] The reductive nature of the substrates could also have induced precipitation of Cu^{2+} as Cu_2O (cuprite) or metallic Cu. Metallic copper nodules have been described in natural wetlands in alpine watersheds in Montana that received pre-historic acid rock drainage.[41,42] However, in the presence of measurable quantities of H_2S, it is certain that any copper or cadmium previously deposited in a carbonate, oxide or elemental state would have quickly tarnished to a sulfide form.

Zinc removal efficiency varied widely from cell to cell, and from season to season, with especially poor performance during the first winter (1996–7). Zinc is thought to have been removed from solution primarily as ZnS, with low removal efficiencies coinciding with decreased hydraulic residence time and low BSR rates.[9] Zinc attenuation was more erratic than copper or cadmium, partly because influent Zn concentrations were much higher (*ca.* 10 mg L^{-1}), and partly because the solubility product of ZnS is greater than that of CdS, CuS or Cu_2S.[38] Manganese removal was nonexistent in winter, although partial attenuation was noted in the anaerobic cells during the summer months. The most likely mechanism for manganese removal in summer was co-precipitation with ZnS (see below), although some Mn may also have been scavenged as impurities in calcite.

Dissolved iron and arsenic levels were generally low in the oxidized influent waters, although particulate Fe and As were sometimes elevated.[30] Slight increases in dissolved Fe and As were noted as the treatment water passed through the anaerobic cells, presumably due to reductive dissolution of ferric oxy-hydroxide compounds and concomitant release of adsorbed arsenic. This was particularly true during the first few months of operation, when concentrations of dissolved arsenic leaving the anaerobic cells were consistently highly elevated (>50 μg L^{-1}).

Adsorption of metals onto organic and inorganic phases in the substrate could have played an important role in the first few months of operation of WDP1. However, extrapolation of the results of adsorption isotherm experiments conducted on substrate materials[35,36] indicate that available adsorption sites probably became saturated in the first 6 months of operation, due to the continuous metal loadings. A similar conclusion was reached for a constructed wetland receiving metal-rich acid mine drainage in Colorado.[2] Likewise, chemical analysis of cattail tissues collected after one year of operation suggests that metabolic uptake of metals by *Typha latifolia* was minimal compared to the total metal loadings.

3.3 Secondary metal particles

Unfiltered metal concentrations at WDP1 were often significantly higher than filtered concentrations,[30] indicating the presence of finely dispersed particles with diameter >0.45 μm (see filtered *vs.* unfiltered zinc, Table 2). This was most evident for As, Cu, and Fe in the influent (oxidized) samples, and Cu, Cd, and Zn in the effluent (reduced) waters. Particles entering the anaerobic cells were chiefly ferric oxy-hydroxides, clays, and organic matter, whereas particles exiting the anaerobic cells were mainly sulfide phases, organics, and detrital grains of calcite, quartz, and other silicate minerals in the gravel substrates. Secondary precipitates near the inlet to cell 2 were orange-brown in color, whereas samples in the interior and near the outlet were black, and smelled of H_2S.

Sulfidic sediments collected in the sampling cups of the internal piezometers from cell 2 were examined by SEM-EDX at the ICAL laboratory, Montana State University. The samples were prepared by pipeting a tiny amount of water-saturated sediment onto a silicon disk, and immediately evacuating with application of a carbon coating. The abundance of detrital mineral fragments and organic material made the process of finding sulfide particles for SEM-EDX analysis somewhat difficult. Best results were obtained by scanning the samples at low power in electron backscatter mode (see also Morse and Cornwell[43]). Clusters of metal sulfide particles appeared as bright spots, due to their higher average atomic mass. Fig. 6 is a backscatter image revealing the distribution of metal sulfide particles on the surface of a sample collected near the outlet to cell 2. This particular field of view had a higher density of sulfide particles than average: nonetheless, sulfide particles were common, and were found in all of the samples examined.

Upon closer examination, the bright spots in Fig. 6 were found to be mainly zinc sulfide particles. Close-up SEM photographs of the ZnS particles are shown in Fig. 7a and 7b. Most of the clusters were on the order of a few tens of micrometers in diameter, and were composed of loosely aggregated spheres approximately 1 μm in diameter, with some larger and some smaller. Farrand[44] produced similar synthetic CuS, FeS and ZnS precipitates, which consisted of spherical particles with diameters from 0.05 to 0.2 μm. The WDP1 precipitates are larger than this. Because the samples were stored for nearly 1 year before SEM examination, it is likely that some ripening occurred, and that the precipitates were initially finer grained. It is significant to note that particles in the 0.05 to 0.4 μm range could have passed through the 0.45 μm membrane filters used in this study to collect water samples.

The approximate composition of the ZnS particles was determined by semi-quantitative EDX analysis, and is summarized in Table 3. Atomic ratios of (Zn + Mn + Fe)/S, Fe/Zn, and Mn/Zn were calculated for each particle. The average ratios were 0.93 ± 0.21, 0.11 ± 0.057, and 0.030 ± 0.0062, respectively (errors represent one standard deviation). The average composition of a zinc sulfide particle

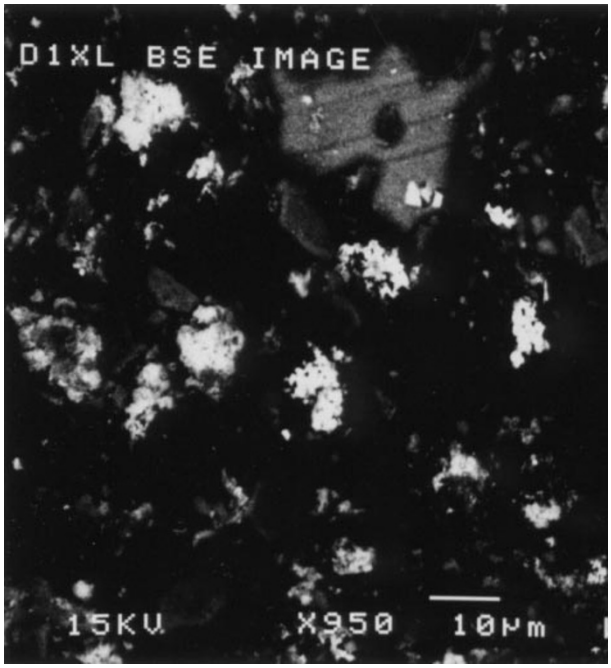

Fig. 6 SEM backscatter image of particles collected near the outlet to cell 2, approximately 4 ft below the surface. The bright spots have a higher mean atomic mass, and are mostly ZnS particles. The darker regions are a mix of organic and mineral matter inherited from the cell substrates.

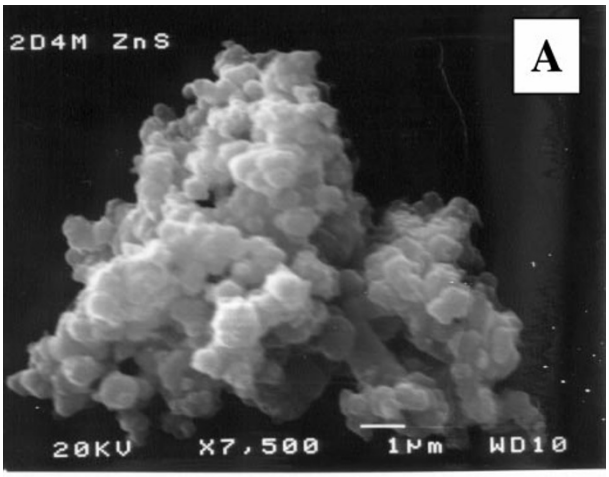

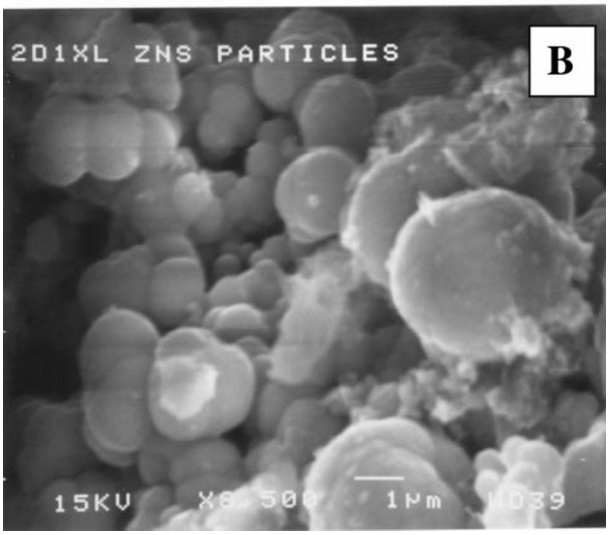

Fig. 7 SEM photomicrographs of ZnS particles collected from cell 2. Note 1 micron bar for scale.

from cell 2 was therefore $(Zn_{0.87}Fe_{0.10}Mn_{0.03})S$. These data indicate that significant and consistent amounts of iron and manganese are present as impurities in the zinc sulfide particles. This is the most likely reason for the aforementioned manganese attenuation in the wetland cells observed in the summer months.

Phase relations in the Zn–Fe–S system[45] indicate that natural sphalerite grains in equilibrium with stoichiometric FeS should

Table 3 EDX compositions of sulfide particles from cell 2

	Atomic%[a]			
Sample	S	Zn	Mn	Fe
2B2L #1	57.0	37.1	1.3	4.6
2B2L #2	55.3	38.2	1.3	5.2
2D1M #4	55.1	39.1	1.2	4.6
2D1XL #1	55.9	40.3	1.1	2.7
2D1XL #2	52.7	43.4	1.1	2.8
2D1XL #3	40.9	51.9	1.6	5.6
2D1XL #5	52.1	44.1	1.5	2.3
2D1XL #6	55.4	34.8	1.2	8.6
2D1XL #7	48.2	44.7	0.8	6.3
2D1XL #8	51.5	43.7	1.6	3.2
2D1M Fe #1[b]	61.8	5.1	—	33.1
2D1M Fe #2[c]	71.2	0.3	1.3	27.2

[a]Compositions normalized to 100%. [b]FeS_x particle, $(Zn + Fe)/S \approx 1 : 1.6$. [c]$FeS_x$ particle, pyrite framboid in Fig. 8, $(Fe + Zn + Mn)/S \approx 1 : 2.5$.

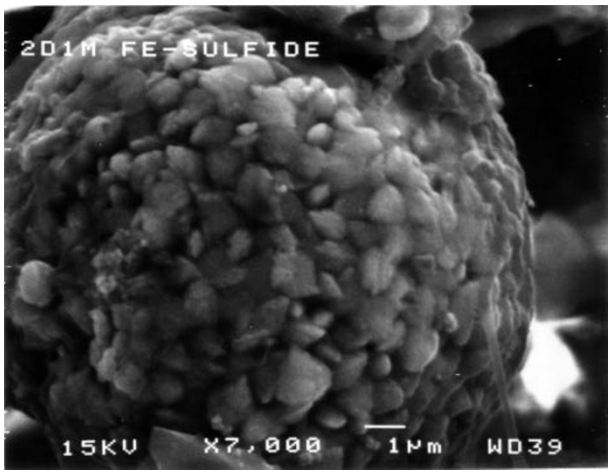

Fig. 8 Fe-sulfide framboid collected from cell 2 substrate. See Table 3 for EDX chemical analysis.

contain approximately 20 mole% FeS. The lower % of Fe in precipitates in WDP1 could be a function of higher redox potentials (FeS-unstable), or could reflect disequilibrium. For example, the high Zn/Fe ratio of influent waters may have locally precluded saturation with a separate Fe-sulfide phase. This is consistent with our observation that Fe-sulfide particles were rare compared to the much more abundant ZnS particles.

Fig. 8 is an SEM photograph of an Fe-sulfide framboid from cell 2. The composition of this particle (Table 3) suggests that it is pyrite. Very similar pyrite framboids have been described from synthesis experiments, as well as from natural environments (*e.g.*, Black Sea sediments).[46,47] Following the reasoning of Wilkin and Barnes,[47] it is likely that the initial Fe-sulfide precipitate in WDP1 was amorphous or crystalline FeS (mackinawite), and that the monosulfide subsequently transformed to pyrite over a period of days to months. This hypothesis is supported by metal solubility constraints (see below). Semi-quantitative EDX analysis indicates that the Fe-sulfide particles contained significant amounts of Mn and Zn (Table 3), although the paucity of data and scatter in the results preclude determination of an average composition. Experimental studies have shown that Mn and Zn can partition into Fe-monosulfide in amounts consistent with our observations.[48,49]

4. Controls on aqueous metal concentrations

The following discussion focuses on the relationship between aqueous sulfide concentration and dissolved metal concentrations at WDP1. A series of diagrams are presented which show filtered metal *vs.* molality of bisulfide. Because pH was approximately constant in the effluent to the anaerobic cells (3 year mean = 6.78, RSD = 0.20), it was not necessary for graphical purposes to portray this variable. Superimposed on each diagram are predicted metal concentrations, based on published experimental studies. These curves were generated from the equilibrium constants listed in Tables 4 and 5, and the measured pH and total dissolved sulfide concentration for each sample. No attempt was made to correct the total dissolved sulfide values for complexation with metals. This problem is discussed below (section 5). Likewise, no attempt was made to adjust the predicted metal solubilities to take into account differences between the actual field temperature and the temperature of the experiment. Such a correction would require accurate information on the temperature dependence of the relevant solubility products and complexation reactions, which in most cases is not available.

For each sample, bisulfide concentration was computed from

the measured pH and total dissolved sulfide values using published values for the dissociation of H_2S. Activity coefficients for dissolved ionic compounds were calculated with MINTEQA2,[50] using the Davies version of the extended Debye–Huckel equation. The ionic strength of water at WDP1 was approximately constant at *ca.* 0.016 (mol kg^{-1}). For these conditions, the computed activity coefficients were 0.88, 0.61, and 0.32, for monovalent, divalent, and trivalent ions, respectively. Uncharged aqueous species were assumed to have an activity coefficient of 1.0.

In the diagrams that follow, results are shown for all analyses in which paired H_2S and filtered metal concentrations were taken at WDP1. Attempts to separate the database according to individual cells showed no meaningful trends, other than the fact that cells 2 and 3 (the cells with compost added) tended to produce more H_2S, whereas cells 1 and 4 tended to have lower H_2S concentrations. For reference, the average dissolved metal concentration of the anaerobic cell influent (*i.e.* the surge pond effluent), is also superimposed on each figure.

4.1 Zinc

Fig. 9 shows various model predictions for ZnS solubility compared with the wetland effluent data. For reference, the analytical detection limit for Zn in the WDP1 study ranged from about 6×10^{-9} to 2×10^{-8} mol kg^{-1}. Predicted solubilities based on the experiments of Daskalakis and Helz[51] and Hayashi *et al.*[52] are virtually identical, and for the conditions of WDP1 are influenced mainly by the following reaction:

$$ZnS_{sphalerite} + H_2S(aq) = Zn(HS)_2(aq) \quad (5)$$

Both of these solubility studies were based on crystalline sphalerite, and appear to underestimate zinc mobility in the WDP1 wetlands, especially at bisulfide concentrations <1 mmol. The two curves labeled MINTEQ in Fig. 9 show the predicted solubility of crystalline (cr) and amorphous (am) ZnS, as predicted using the MINTEQ database. The MINTEQ estimates have a similar shape to those of ref. 50 and 51, with amorphous ZnS being *ca.* 2.5 log units more soluble than crystalline ZnS. Gubeli and Ste. Marie[53] measured the

Table 4 Selected thermodynamic data for the Fe–S, Zn–S, Cu–S, and Cd–S systems

Source	Solid	T/°C	Reactions	Log K
65	Amorphous FeS	20	$FeS + H^+ = Fe^{2+} + HS^-$	−3.00
			$FeS + H^+ + HS^- = Fe(HS)_2^\circ$	+3.45
51	Crystalline sphalerite	25	$ZnS + H_2S^\circ = Zn^{2+} + 2HS^-$	−18.47
			$ZnS + H_2S^\circ = Zn(HS)_2^\circ$	−5.65
			$ZnS + 2HS^- = ZnS(HS)_2^{2-}$	−5.33
			$ZnS + H_2S^\circ + 2HS^- = Zn(HS)_4^{2-}$	−3.83
			$ZnS + HS^- = ZnS(HS)^-$	−4.64
52	Crystalline sphalerite	25	$ZnS + H_2S^o = Zn(HS)_2^\circ$	−5.3
			$ZnS + H_2S^o + HS^- = Zn(HS)_3^-$	−3.3
			$ZnS + H_2S^o + 2HS^- = Zn(HS)_4^{2-}$	−3.4
			$ZnS + H_2O + HS^- = Zn(OH)(HS)_2^-$	−4.4
			$ZnS + H_2O + 2HS^- = Zn(OH)(HS)_3^{2-}$	−4.9
53	Amorphous ZnS	25	$ZnS + H^+ = Zn^{2+} + HS^-$	−10.89[a]
			$ZnS + H_2O = Zn(OH)(HS)^\circ$	−5.87
54	Crystalline covellite, CuS	25	$CuS + H^+ = Cu^{2+} + HS^-$	−20.95
			$CuS + 2HS^- = CuS(HS)_2^{2-}$	−4.97
			$CuS + 3HS^- = CuS(HS)_3^{3-}$	−4.04
			$CuS + 4S(s) + HS^- = CuS(S_5)^{2-} + H^+$	−12.19[b]
			$CuS + 6.5S(s) + 1.5HS^- = CuS_4S_5^{3-} + 1.5H^+$	−15.71[c]
			$CuS + 7.5S(s)\ 1.5HS^- = Cu(S_5)_2^{3-} + 1.5H^+$	−16.06[c]
55	Crystalline chalcocite, Cu_2S	22	$Cu_2S + H^+ = 2Cu^+ + HS^-$	−34.62
			$0.5Cu_2S + 1.5HS^- + 0.5H^+ = Cu(HS)_2^-$	−0.13
			$Cu_2S + 2HS^- = Cu_2S(HS)_2^{2-}$	−4.75
10	Crystalline greenockite (gr) and two amorphous precipitates (a1 and a2)	25	$CdS(gr) + H^+ = Cd^{2+} + HS^-$	−14.82
			$CdS(a1) + H^+ = Cd^{2+} + HS^-$	−14.40
			$CdS(a2) + H^+ = Cd^{2+} + HS^-$	−14.15
			$Cd^{2+} + HS^- = Cd(HS)^+$	+7.38
			$Cd^{2+} + 2HS^- = Cd(HS)_2^\circ$	+14.43
			$Cd^{2+} + 3HS^- = Cd(HS)_3^-$	+16.28
			$Cd^{2+} + 4HS^- = Cd(HS)_4^{2-}$	+18.43
63	Crystalline greenockite	25	$CdS + H^+ = Cd^{2+} + HS^-$	−14.36
			$Cd^{2+} + 3HS^- = Cd(HS)_3^-$	+16.44
			$Cd^{2+} + 4HS^- = Cd(HS)_4^{2-}$	+17.89
			$Cd^{2+} + HS^- + H_2O = CdOHS^- + 2H^+$	−2.47
62	Amorphous CdS	25	$CdS + H^+ = Cd^{2+} + HS^-$	−12.28[d]
			$Cd^{2+} + HS^- = Cd(HS)^+$	+7.55
			$Cd^{2+} + 2HS^- = Cd(HS)_2^\circ$	+14.61
			$Cd^{2+} + 3HS^- = Cd(HS)_3^-$	+16.49
			$Cd^{2+} + 4HS^- = Cd(HS)_4^{2-}$	+19.35

[a]Adjusted from S^{2-} using Gubeli's[53] dissociation constant: $HS^- = H^+ + S^{2-}$, log K = −13.48. [b]Adjusted using the reaction from Shea and Helz:[58] $4S(s) + HS^- = S_5^{2-} + H^+$, log K = −9.44. [c]Adjusted using the reaction from Shea and Helz:[58] $3S(s) + HS^- = S_4^{2-} + H^+$, log $K = -9.56$. [d]Adjusted from S^{2-} using Ste. Marie's[62] dissociation constant: $HS^- = H^+ + S^{2-}$, log $K = -13.48$.

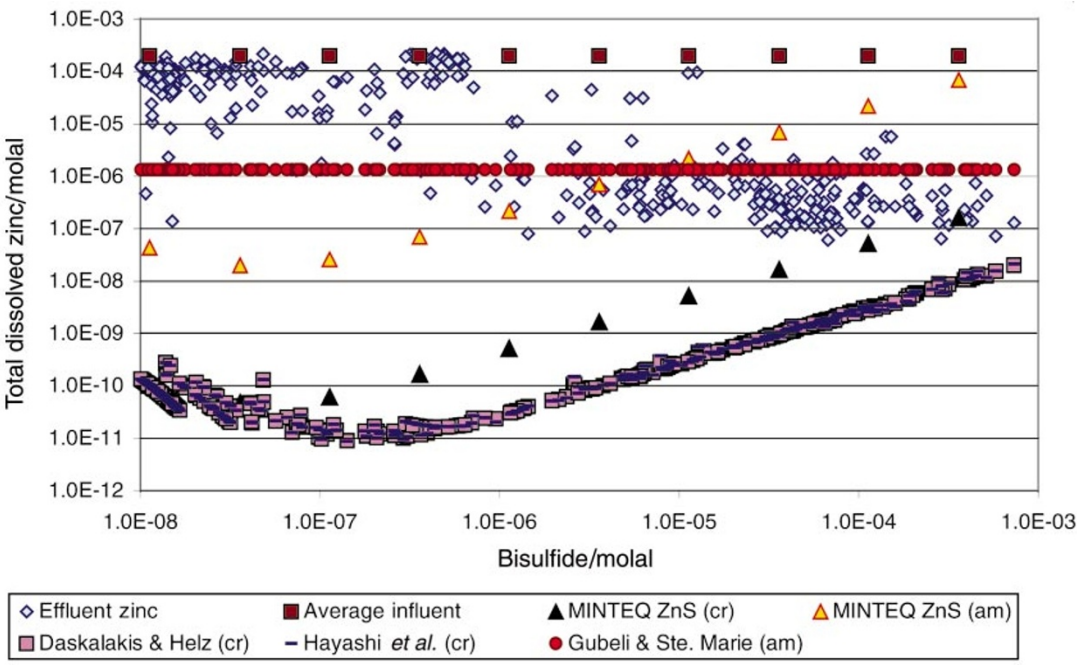

Fig. 9 Comparison of concentrations of filtered zinc at WDP1 *vs.* predicted values based on solubility models from literature sources.

solubility of freshly precipitated (amorphous) ZnS as a function of dissolved sulfide (0.004 to 0.01 molar) and pH (1 to 14). ZnS solubility was independent of both variables at pH > 3, being constant at *ca.* 1.3×10^{-6} mol kg^{-1}. To explain these observations, Gubeli and Ste. Marie proposed the following reaction:

$$ZnS_{amorphous} + H_2O = Zn(HS)(OH)(aq) \quad (6)$$

Of the previous studies investigated, the flat nature of the WDP1 data at sulfide concentrations $>10^{-6}$ mol kg^{-1} is best matched by the results of Gubeli and Ste. Marie.[53] Both data sets are independent of bisulfide concentration, and have comparable solubility values. However, Daskalakis and Helz[51] have argued that the constantly elevated Zn concentrations measured by Gubeli and Ste. Marie were due to the presence of colloidal ZnS particles. It is possible that colloidal ZnS particles could have passed through the filters used by Gubeli and Ste. Marie (filter size not specified), and also the samples taken in this study (0.45 μm filter). This idea is discussed in greater detail below.

4.2 Copper

The behavior of copper in sulfidic solutions is complicated by the possibility of multiple valence states, *i.e.*, $Cu^{(I)}$ *vs.* $Cu^{(II)}$. Here, we compare the WDP1 results with solubility models of Shea and Helz,[54] and Mountain and Seward.[55] Shea and Helz assumed that all dissolved copper in their experiments was in the cupric form, that covellite (CuS) was the stable sulfide mineral, and that aqueous complexes formed with both dissolved sulfide and polysulfide compounds (Table 4). On the other hand, Mountain and Seward presented a model in which all dissolved copper is in the cuprous valence, chalcocite (Cu_2S) is the stable sulfide mineral, and only sulfide complexes are present (*e.g.*, $Cu(HS)_2^-$). Mountain and Seward pointed out that the electrochemical potential required for the reduction of sulfate to sulfide (−0.21 V at pH 7) is much lower than the potential for the reduction of $Cu^{(II)}$ to $Cu^{(I)}$ (+0.16 V), making $Cu^{(II)}$ incompatible with dissolved sulfide. Nonetheless, aqueous $Cu^{(II)}$ sulfide complexes could persist if they are unusually stable, or if transformation of $Cu^{(II)}$ to $Cu^{(I)}$ was kinetically inhibited. Some combination of the two models is also possible. For example, $Cu^{(I)}$ sulfide complexes could exist in equilibrium with covellite, or $Cu^{(II)}$ with chalcocite. Equilibrium between the two copper sulfide phases may be written as follows:

$$0.5Cu_2S_{chalcocite} + 0.5S(s) = CuS_{covellite} \quad (7)$$

$$0.5Cu_2S_{chalcocite} + 0.5H_2S(aq) = CuS_{covellite} + H^+ + e \quad (8)$$

Reaction (7) has a calculated free energy change of −3.75 kcal mol^{-1},[56] indicating that covellite is the stable copper sulfide in the presence of elemental sulfur. In the absence of sulfur, the relative stability of the two phases depends on the Eh, pH and H_2S concentration (reaction 8). Using thermodynamic data,[56] it can be shown that covellite is the stable phase for the conditions of the WDP1 anaerobic cells (pH *ca.* 7, Eh *ca.* −200 mV, $H_2S > 10^{-6}$ mol kg^{-1}). Also, at this Eh, aqueous Cu^+ should predominate over Cu^{2+}.

To calculate the concentrations of the $Cu^{(II)}$ polysulfide complexes proposed by Shea and Helz,[54] it was assumed that solid elemental sulfur was present in the WDP1 cells, with an activity of unity. Although elemental sulfur was not directly observed in subsurface water samples, it was present in abundance in cells 6 and 7 near the outlet to the anaerobic cells. It is reasonable to assume that elemental sulfur particles were also forming in the subsurface, due to mixing of water from different micro-environments, diffusion of oxygen from the atmosphere, and/or respiration of oxygen by cattails and other plants in the root zone.[57] In the event that the subsurface waters were undersaturated with elemental sulfur, the estimated solubilities based on the model of Shea and Helz[54] are still useful in that they provide a maximum limit on the stability of $Cu^{(II)}$ polysulfide complexes.

Fig. 10 shows the predicted copper solubility trends compared with wetland effluent data. The detection limit for Cu ranged from 9×10^{-9} to 2×10^{-8} mol kg^{-1}. The majority of measured Cu concentrations were more than one order of magnitude above the IDL. The models based on Mountain and Seward[55] and Shea and Helz[54] appear to match the data from WDP1 fairly well at the upper range of bisulfide concentrations presented. However, the two models significantly diverge from each other at lower sulfide concentrations, and both underestimate the WDP1 field data. To explain this discrepancy, a number of possibilities are considered. First, it is possible that

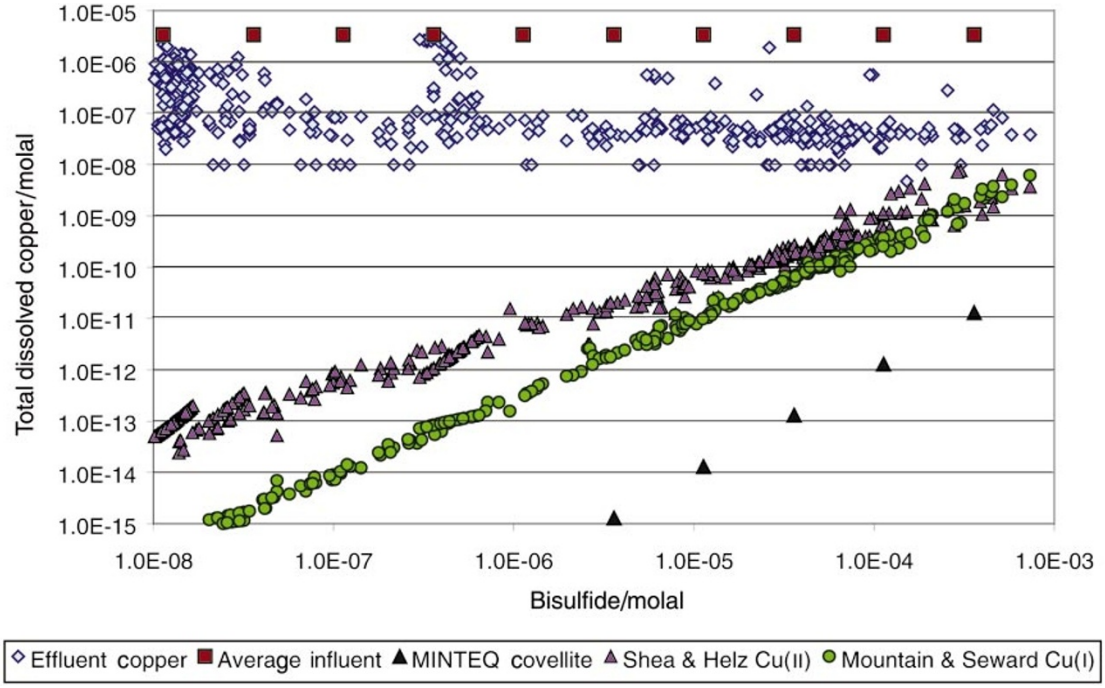

Fig. 10 Comparison of concentrations of filtered copper at WDP1 *vs.* predicted values based on solubility models from literature sources.

copper concentrations at WDP1 were controlled by a metastable or poorly crystalline phase. Shea and Helz[58] reported that the solubility of poorly crystalline copper monosulfide (approximate composition $Cu_{1.18}S$) was roughly three orders of magnitude greater than that of crystalline covellite. Also, Thompson and Helz[59] proposed that chalcocite can metastably control dissolved copper in sulfidic waters in cases where covellite is predicted to be the stable solid phase. Thompson and Helz showed that deep Black Sea water was *ca.* 2 to 2.5 orders of magnitude supersaturated with respect to covellite, but close to equilibrium saturation with chalcocite. The main problem with invoking amorphous or metastable Cu–S phases to explain the WDP1 data is that, although the solubilities of these phases are much higher than crystalline covellite, there still should exist a positive correlation between total dissolved copper and total dissolved sulfide. Such a correlation is absent in the WDP1 data shown in Fig. 10.

It is also quite possible that the elevated copper concentrations at WDP1 were due to sampling of colloidal Cu-sulfide particles with diameter < 0.45 μm. Cu-sulfide sols formed by rapid precipitation with H_2S have been described,[60,61] and it has been suggested that the sulfide nanocrystals in these sols may remain in suspension for years, provided the total metal concentration and ionic strength are both low.[60] This hypothesis would explain the relatively high concentration of copper in filtered samples, as well as the lack of influence of copper mobility on dissolved sulfide shown in Fig. 10.

4.3 Cadmium

The cadmium-sulfide system is similar to zinc in that Cd does not undergo a valence reduction in the presence of sulfide. Thermodynamic data for solubility reactions involving crystalline CdS (greenockite) and amorphous CdS are summarized in Table 4. Fig. 11 shows the predicted cadmium solubility trends based on these data, compared with the WDP1 data. Cadmium was removed quite effectively in the anaerobic wetland cells. Because most analyses were at or near the instrument detection limit (9×10^{-10} to 1×10^{-8} mol kg^{-1}), the apparent straight lines formed by the WDP1 data are possibly an artifact of analytical shortcomings. The predictions for cadmium solubility in the presence of sulfide are well below the analytical detection limits.

The same general solubility model for CdS was derived from the experiments of Wang and Tessier[10] and Ste. Marie *et al.*[62] In both studies, all of the complexes of interest had the general formula $Cd(HS)_x^{2-x}$, and similar dissociation constants were obtained. The curve generated from MINTEQ also reflects the general shape of these models. For reasons that are not

Table 5 Thermodynamic data for the As–S system

Source	Solid	T/°C	Reactions	Log K
67	Crystalline orpiment	22	$As_2S_3 + 6H_2O = 2H_3AsO_3^\circ + 3H_2S$	−25.8
68	Crystalline orpiment	22	$As_2S_3 + H_2O = H_2As_2S_3O^\circ$	−6.45
			$As_2S_3 + HS^- = HAs_2S_4^-$	−1.47
			$As_2S_3 + OH^- + HS^- = As_2S_4^{2-} + H_2O$	+4.05
69	Crystalline orpiment	25	$0.5As_2S_3 + 3H_2O = H_3AsO_3^\circ + 1.5HS^- + 1.5H^+$	−23.11
			$1.5As_2S_3 + 1.5HS^- + 0.5H^+ = H_2As_3S_6^-$	+3.61
70	Amorphous As_2S_3	25	$0.5As_2S_3 + 3H_2O = H_3AsO_3^\circ + 1.5H_2S^\circ$	−11.9
			$1.5As_2S_3 + 1.5H_2S^\circ = H_2As_3S_6^- + H^+$	−5.0
71	Amorphous As_2S_3	25	$0.5As_2S_3 + 3H_2O = H_3AsO_3^\circ + 1.5HS^- + 1.5H^+$	−22.38
			$1.5As_2S_3 + 1.5HS^- = As_3S_5(SH)^{2-} + 0.5H^+$	+1.78
			$1.5As_2S_3 + 1.5HS^- = 1.5H^+ = HAs_3S_4(SH)_2^\circ$	+14.74

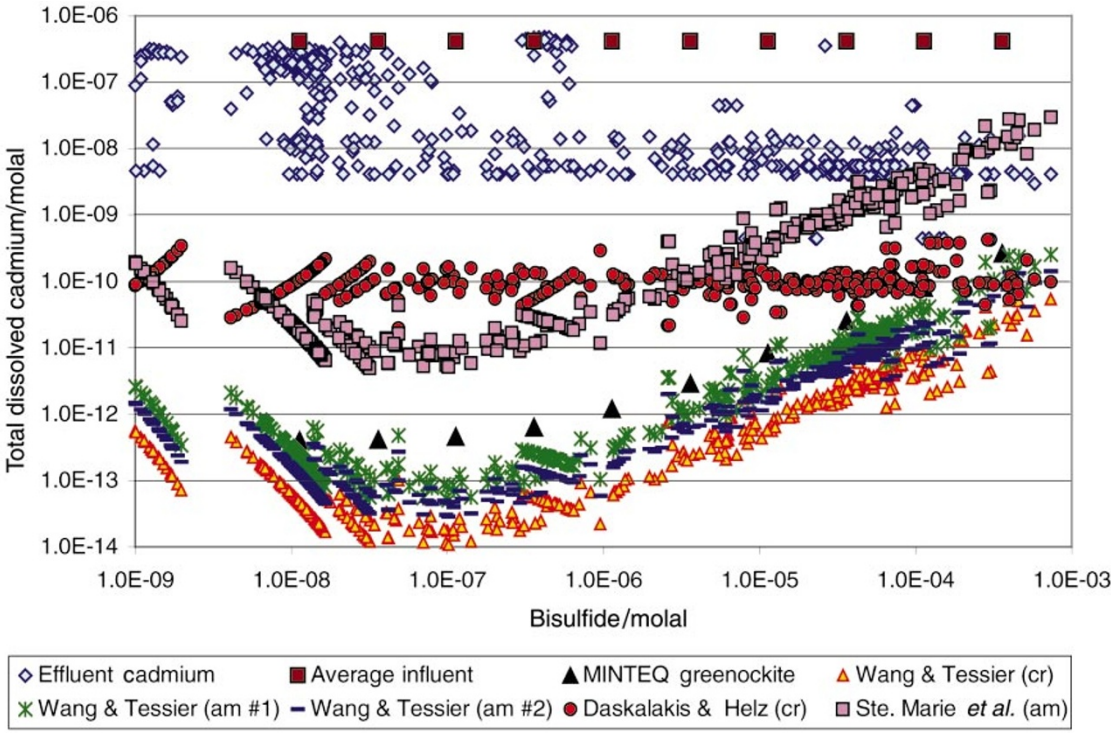

Fig. 11 Comparison of concentrations of filtered cadmium at WDP1 *vs.* predicted values based on solubility models from literature sources.

obvious, amorphous CdS from Ste. Marie *et al.* is about two orders of magnitude more soluble than the amorphous phase in Wang and Tessier. The curve representing the model by Daskalakis and Helz[63] has a different shape, reflecting the fact that the dominant aqueous species using their data for the conditions of WDP1 is a mixed hydroxy-sulfide complex, $CdOHS^-$.

4.4 Iron

Iron entered the WDP1 wetland primarily as suspended ferric oxyhydroxides.[34,36] In the anaerobic cells, iron presumably underwent bacterial reduction to aqueous $Fe^{(II)}$, some of which subsequently precipitated as a sulfide. Because influent Zn/Fe ratios were very high (>100, see Table 2), most of the attenuated iron can be accounted for as impurities in ZnS. Additional Fe-sulfide precipitates could have formed *in situ* by sulfidation of Fe-bearing oxide and silicate minerals present in the original river gravel substrates. For the purposes of this study, it was assumed that the first iron sulfide mineral formed was amorphous FeS. Over time, this phase could have converted to other more stable iron sulfide minerals such as mackinawite (tetragonal FeS), greigite (cubic Fe_3S_4), and eventually pyrite (FeS_2).[64] However, experimental and modeling studies indicate that the rapidly formed amorphous FeS phase often controls dissolved iron and dissolved sulfide concentrations in natural sulfidic waters.[65]

Fig. 12 shows the predicted iron solubility trends according to the data in the recent compilation of Davison *et al.*,[65] as compared with the WDP1 wetland effluent data. The detection limit for Fe ranged from about 9×10^{-9} to 3×10^{-8} mol kg^{-1}. The models of Davison *et al.* and MINTEQA2, based upon amorphous FeS solid phases, bracket the observed iron concentrations well once bisulfide concentrations exceed *ca.* 5×10^{-5} mol kg^{-1}. At lower sulfide concentration, it is likely that iron solubility in the wetland cells was limited by ferric oxide/hydroxide phases. For the following reactions:

$$Fe(OH)_3(\text{ferrihydrite}) + H_2S(aq) + H^+ + e^- = FeS(am) + 3H_2O(l) \quad (9)$$

$$FeOOH(\text{goethite}) + H_2S(aq) + H^+ + e^- = FeS(am) + 2H_2O(l) \quad (10)$$

Log K at 25 °C is computed to be 14.84 and 8.95, respectively.[64,66] Assuming pH = 7 and Eh = −200 mV (a reasonable value for neutral waters containing small amounts of sulfide), ferric oxy-hydroxide should convert to amorphous FeS at H_2S concentrations greater than 3×10^{-11} mol kg^{-1} (ferrihydrite-stable) or greater than 2×10^{-5} mol kg^{-1} (goethite stable). A comparison of these values with Fig. 12 suggests that goethite may be the solubility-limiting phase for iron in the anaerobic cells when H_2S concentrations are less than roughly 10^{-5} mol kg^{-1}. In contrast, ferrihydrite (poorly crystalline ferric hydroxide) is predicted to sulfidize to FeS at extremely low H_2S concentrations.

Unlike zinc and copper, ferrous iron does not undergo significant complexation with bisulfide until the concentration of the latter exceeds about 10^{-3} mol kg^{-1},[65] which is near the upper limit of the measured values at WDP1.

4.5 Arsenic

Of all the metals considered in this study, the arsenic sulfide system is the least well constrained. Small amounts of arsenic entered the wetland primarily in particulate form, presumably as $As^{(v)}$ adsorbed to ferric oxyhydroxide particles in the Metro Storm Drain. As the iron particles underwent reductive dissolution and/or sulfidation in the anaerobic cells, it is likely that adsorbed arsenic was released and subsequently reduced to $As^{(III)}$. In the presence of very high amounts of H_2S, it is possible that some arsenic may have been attenuated in sulfide form. This is discussed below.

Selected thermodynamic data for the arsenic-sulfide system are presented in Table 5. Considerable disagreement persists over the exact nature of the arsenic sulfide complexes. In particular, it is uncertain whether the complexes exist as

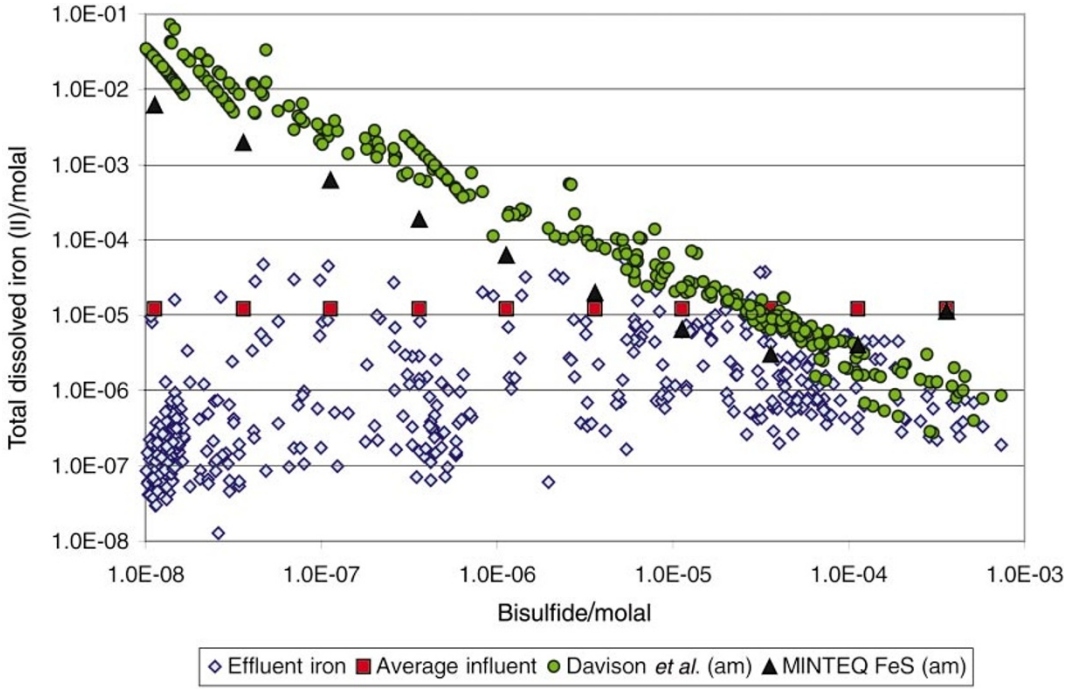

Fig. 12 Comparison of concentrations of filtered iron at WDP1 *vs.* predicted values based on solubility models from literature sources.

monomers, dimers, or trimers. Mironova *et al.*[67,68] proposed dimeric complexes. The other authors advocate monomers or trimeric arsenic sulfide complexes. Models by Webster[69] and Eary[70] include the same suite of trimeric complexes, but differ in the crystallinity of the solid phase. Young and Robins[71] obtained very high solubilities for amorphous As_2S_3 in H_2S solutions (solubility minimum = 45 ppm), and proposed yet another set of polynuclear aqueous complexes. Helz *et al.*[72] argued that, whereas polynuclear As-sulfide complexes probably dominate in As_2S_3-saturated solutions, mononuclear complexes are more likely at the low As concentrations of most natural waters.

Fig. 13 shows the predicted arsenic solubility trends compared with wetland effluent data. The average influent arsenic concentration is shown for reference. The detection limit for arsenic ranged from about 1×10^{-8} to 3×10^{-8} mol kg^{-1}. In contrast to the metals discussed previously, the WDP1 data do not show arsenic removal as a function of increased sulfide concentration. Instead, a slight increase is observed at higher bisulfide concentrations, indicating mobilization rather than attenuation in the anaerobic cells. The increase in dissolved arsenic concentrations is attributed to dissolution of particulate or adsorbed arsenic from the influent water, or dissolution of trace amounts of arsenic present in the original gravel substrates themselves.

Arsenic solubility curves in Fig. 13 based upon crystalline and amorphous As_2S_3 show that the WDP1 waters are significantly undersaturated with respect to these solid phases. In contrast to the other metals of concern, precipitation of As_2S_3 is not a viable mechanism to remove dissolved arsenic to regulatory standards. For example, the Montana drinking

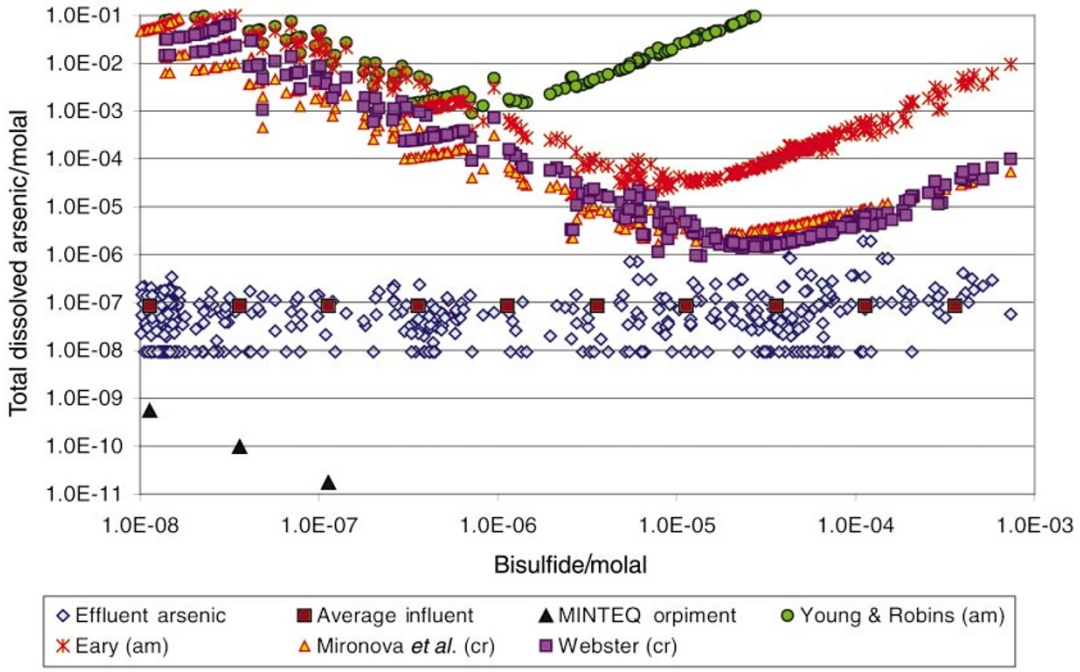

Fig. 13 Comparison of concentrations of filtered arsenic at WDP1 *vs.* predicted values based on solubility models from literature sources.

water standard for arsenic is 18 ppb,[73] and the EPA maximum contaminant level is 50 ppb (this may drop pending research and legislation in progress). Both of these values are below the minimum predicted solubility of As_2S_3 based on the various models shown in Fig. 13. The undersaturation of WDP1 waters with As_2S_3 is therefore explained by a combination of high solubility and low influent As concentrations. It is also possible that arsenic levels were kept low by adsorption or co-precipitation of arsenic onto Zn- and Fe-sulfide phases. However, we have no evidence for this mechanism.

4.6 Manganese

Compared to the metals discussed previously, the aqueous and solid forms of manganese sulfide are relatively unstable, and probably played an insignificant or minor role at WDP1. The concentration of dissolved manganese in the anaerobic cells was far less than what would be predicted from the recommended solubility product of MnS. However, it is obvious from section 3.3 that some manganese was co-precipitated with ZnS. Most of this attenuation occurred during the mid-summer months, when H_2S concentrations were highest. It is possible that manganese was removed as a partial solid solution in ZnS, based on the relatively uniform composition (*ca.* 3 mole% MnS) of the ZnS particles analyzed. For the following reaction:

$$MnS(am) + H^+ = Mn^{2+} + HS \quad (11)$$

Log K (25 °C) is estimated at $+3.8$.[66] If we assume ideal mixing, the activity of MnS in the ZnS particles of WDP1 would be roughly 0.03. Using this value, and the measured pH, bisulfide and manganese concentrations, the WDP1 waters are still undersaturated with MnS by >1 log unit. Thus, unless the MnS–ZnS solution is strongly non-ideal, it is more likely that manganese was removed by a non-equilibrium co-precipitation process, or by adsorption onto freshly precipitated ZnS particles.

4.7 Metal organic complexes

Given the abundance of solid organic matter in the substrates for the anaerobic cells at WDP1, the possible importance of organic ligands should be considered. Dissolved organic carbon (DOC) was monitored on a regular basis at the outlet to each anaerobic cell. DOC values were usually low year-round, falling in the range of 0 to 10 mg L^{-1} (as C). These levels probably reflect a balance between DOC production by plants and fermentative bacteria, and DOC consumption by heterotrophic bacteria (such as iron and sulfate reducing bacteria). Rarely, during brief periods of time, DOC concentrations in the WDP1 cells showed anomalous increases to values $>$ 50 mg L^{-1}. These episodes occurred when drastic reductions in flow rate—and corresponding increases in residence time—allowed BSR reactions to continue to the point where most of the dissolved sulfate of influent waters was consumed. Once sulfate dropped below a certain threshold level, BSR rates decreased, allowing soluble organic compounds to accumulate *via* fermentation and methanogenesis.[74]

Even at the more elevated DOC levels discussed above, it is exceedingly unlikely that organic ligands could out-compete with bisulfide for most of the metals of concern. For example, for the following reactions, (where Ac = acetate):

$$Zn^{2+} + 2HS^- = Zn(HS)_2(aq) \quad (12)$$

$$Zn^{2+} + 2Ac^- = Zn(Ac)_2(aq) \quad (13)$$

the respective log β_2 values are $+12.82$[51] and $+3.45$.[75] The ligand exchange reaction can be written:

$$Zn(Ac)_2(aq) + 2HS = Zn(HS)_2(aq) + 2Ac \quad (14)$$

for which log $K = +9.37$. The condition $\{Zn(Ac)_2\} = \{Zn(HS)_2\}$ would require $\log(Ac^-/HS^-) = 4.68$. In other words, for the Zn–acetate complex to be important, acetate would need to be roughly 4 orders of magnitude more abundant than bisulfide. This was rarely the case for the WDP1 waters, even if we make the exceedingly unlikely assumption that 100% of the measured DOC was present as acetate. A similar conclusion can be made comparing the stability of sulfide *vs.* acetate complexes for cadmium and copper. Although organic complexation of iron, manganese and arsenic is potentially more important, no correlation was noted in this study between DOC and these metals.

5. Discussion

Most of the solubility models presented above generate a "U-shaped" solubility curve over a sufficiently wide range in sulfide concentration (*e.g.*, see Fig. 1). However, the field data from WDP1 clearly do not show this type of behavior. Instead of a U-shaped curve, we see a tendency for metal concentrations in the presence of H_2S to be buffered to a nearly constant value. The geometric mean values and standard deviations for each metal are summarized in Table 6, and are based on all data entries in the WDP1 database for aqueous sulfide concentrations $>10^{-6}$ mol kg^{-1}. With the possible exception of zinc (see section 4.1), it is difficult to reconcile the flat solubility dependencies with the experimental results.

One possible explanation for the discrepancy between the field and laboratory data is that additional aqueous complexes are present in the waters of WDP1 for which thermodynamic data are unavailable. In this respect, it is important to realize that most of the previous solubility experiments were conducted at relatively high total sulfide concentrations. For example, the lowest total sulfide values used by Shea and Helz,[54] Mountain and Seward,[55] and Daskalakis and Helz[51] were 0.001, 0.01 and 0.0004 mol kg^{-1}, respectively. Thus, the maximum sulfide concentrations measured in the WDP1 treatment wetland (which are similar to the upper limit of H_2S in natural sulfidic waters) are at the lower end of the range of total sulfide employed in the experimental studies. In general, the lack of experimental information at low ligand concentration is a common problem in solubility studies: in order to obtain quantities of reactants and products that can be accurately measured, it is often necessary to perform experiments at unrealistically high ligand concentrations. Although procedurally difficult, further experiments are needed to more closely mimic the conditions of natural sulfidic waters.

It is also possible that the nearly constant and elevated metal concentrations obtained from WDP1 are due to sampling of metal-sulfide colloid or cluster compounds. It is widely known that colloidal ZnS sols form during rapid precipitation of Zn-sulfide from aqueous solution. Daskalakis and Helz[51] found that colloidal ZnS particles persisted for at least several days, and that the aged solutions did not equilibrate with crystalline sphalerite, even after several months. To obtain equilibrium solubility values, Daskalakis and Helz went to great lengths to avoid supersaturation (they could not reverse their experi-

Table 6 Concentration of filtered metals at WDP1 in presence of H_2S

Metal	Mean (log mol kg^{-1})	n	Standard deviation	Range of H_2S
Zn	−6.2	81	0.6	10^{-6} to 10^{-3} mol kg^{-1}
Cu	−7.4	81	0.5	10^{-6} to 10^{-3} mol kg^{-1}
Cd	−8.2	81	0.5	10^{-6} to 10^{-3} mol kg^{-1}
Fe	−5.6	81	0.5	10^{-6} to 10^{-3} mol kg^{-1}
As	−6.7	81	0.6	10^{-6} to 10^{-3} mol kg^{-1}

ments), lest colloids were allowed to form and persist. Along the same lines, Luther *et al.*[76] discuss the formation of aqueous zinc sulfide clusters that form at relatively low concentrations of metal and bisulfide. Their results indicate that these clusters are precursors to solid precipitate formation, and are "thermodynamically strong". Similar copper sulfide sols have been shown to be stable for years, depending on the solution pH, metal concentration, and ionic strength.[60,61] Rozan *et al.*[77] describe sulfide cluster compounds containing zinc, iron and copper with diameters < 0.2 μm in oxic, polluted rivers in the eastern US. These compounds apparently persist for days, even in the presence of oxygen, and can contribute to "dissolved" metal concentrations of up to 6×10^{-7} mol kg^{-1}, which, coincidently, is close to the filtered copper and zinc concentrations obtained from the WDP1 wetlands (Table 6). It is very possible that similar colloidal metal sulfide particles could form and persist over the time frame of a rapid treatment scheme such as WDP1. The very cold water temperatures in the winter months could have further retarded flocculation and growth of sulfide particles to filterable dimensions. Ultra-filtration to 0.001 μm would have been necessary to discriminate between colloidal *vs.* dissolved metal, but even this pore size would not filter out the cluster compounds proposed by Luther *et al.*[76] and Rozan *et al.*[77] such as M_2S_4, M_3S_3, and M_4S_6 (M = Cu, Fe, or Zn). No attempts to collect ultra-filtered samples were made at WDP1 during its life of operation.

A third factor to consider regarding the discrepancy between field and experimental results deals with the quality of the WDP1 data. With the exception of cadmium, all of the metals discussed in this paper were typically well above their instrument detection limits. There is, however, considerable error associated with the dissolved sulfide measurements at the lower range of values reported ($< 10^{-5}$ mol kg^{-1}). For one thing, the instrument detection limit for the colorimetric procedure employed is on the order of 10^{-7} to 10^{-8} mol kg^{-1} S^{2-}, and the suggested method detection limit quoted by HACH is even higher (*ca.* 3×10^{-7} mol kg^{-1}). Because sulfide was not a priority analyte, no rigorous quality control procedures were performed at WDP1 to test the accuracy or precision of the analytical results at very low sulfide concentrations. A second problem is that, in some cases, a significant amount of the total sulfide measured during the colorimetric determination could have been initially complexed with dissolved metal. Mass balance calculations indicate that the only metal in this study that could significantly influence the total sulfide mass balance at low S^{2-} concentrations is zinc. The geometric mean concentration of dissolved zinc for 81 samples with total sulfide $> 10^{-6}$ mol kg^{-1} was 6.3×10^{-7} mol kg^{-1} (Table 6). Even at very low sulfide concentrations, the data of Daskalakis and Helz[51] suggest that the dominant aqueous zinc complex was $Zn(HS)_2^-$. If so, this implies that *ca.* 10^{-6} mol kg^{-1} of dissolved sulfide could easily have been tied up as an aqueous zinc complex. Thus, the true concentration of "free" sulfide may have been overestimated in Fig. 9 to 13, especially at $\Sigma S^{2-} < 10^{-5}$ mol kg^{-1}. To make matters worse, Thompson and Helz[59] have shown that S^{2-}/Zn mole ratios near unity favor the formation of ZnS cluster particles, which for the most part have not been thermodynamically well-characterized. This is analogous to the polymerization of metal cations undergoing hydrolysis, where the final Me/OH ratios are near unity.[78]

Finally, it is instructive to re-examine the possible errors introduced from two of the more dubious assumptions made in our solubility calculations. Firstly, the calculations assumed pure phases, whereas it is possible or indeed likely that the sulfide particles consisted of solid solutions or intimately mixed precipitates. Incorporation of a solid solution model would lower the activity of the end-member metal sulfide component, resulting in lower calculated solubilities. For zinc, copper and cadmium, this would only worsen the agreement between observed and theoretical dissolved concentrations. For arsenic and manganese, the gap would be lessened, although probably not enough to result in a close agreement (see section 4.6). The second assumption of a uniform temperature of 25 °C also needs to be examined. The WDP1 water was typically much cooler than 25 °C, approaching 0°C in the winter months. Unfortunately, recalculation to the true field temperature was not possible in this study, because accurate data on the temperature dependence of the relative solubility-controlling reactions (including formation constants for individual metal sulfide complexes) are missing or incomplete. However, a rough idea of the direction and possible magnitude of the temperature correction can be obtained by examination of the enthalpies of the solubility products of each metal sulfide system. Expressed in the following format:

$$MeS + H^+ = Me^{2+} + HS^- \qquad (15)$$

the standard enthalpies of reaction (15) for crystalline ZnS, CuS, CdS, and MnS are $+34.5$, $+100.5$, $+68.5$ and -24.2 kJ mol^{-1}, respectively.[66] Thus, for zinc, copper and cadmium, sulfide mineral dissolution is endothermic, and will decrease with decrease in temperature, whereas the reverse is true for manganese. Using a Van't Hoff extrapolation of the above solubility product of sphalerite, a drop in temperature from 25 to 2 °C translates into a drop in the theoretical zinc solubility of just under one order of magnitude. This will worsen the discrepancy between our calculated Zn solubilities and the observed concentrations in the field. This is also true for most of the other metals of interest, including manganese, which was shown to be strongly undersaturated with respect to pure MnS.

6. Conclusions

This paper has examined in some detail the interactions between metals and dissolved sulfide in a treatment wetland. The results are applicable to other treatment facilities employing bacterial sulfate reduction, as well as natural wetlands receiving anomalous metal loadings. From this study, it is clear that the processes involved are complex and incompletely understood. Because of the large number of unanswered questions, a few recommendations are offered for further work. First, continued experiments are needed in low temperature, aqueous metal sulfide systems to resolve the various discrepancies between published laboratory studies, as well as the discrepancies between field *vs.* experimental results. In particular, experiments are needed which employ the low sulfide concentrations and poorly crystalline compounds typical of natural environments. Experiments are also needed to test the effect of temperature on the solubility of amorphous metal sulfide phases. Finally, future case studies of metals in sulfidic waters should make a concerted attempt to discriminate between dissolved *vs.* colloidal metal transport. Unfortunately, knowledge of the precise chemical mechanisms attending a particular water treatment system is often of secondary importance to individuals who are mainly concerned with the overall system performance (*e.g.*, Table 2 or Table 6). To a system operator, it may be of little consequence whether copper, zinc, and cadmium are present in dissolved *vs.* colloidal form (for example), as long as regulatory standards for discharge water quality are met. However, generalization of the results from one project to another site will ultimately require knowledge of the fundamental processes responsible for metal attenuation.

References

1 S. D. Machemer, J. S. Reynolds, L. S. Laudon and T. R. Wildeman, Balance of S in a constructed wetland built to treat acid mine drainage, Idaho Springs, Colorado, USA, *Appl. Geochem.*, 1993, **8**, 587.

2 S. D. Machemer and T. R. Wildeman, Adsorption compared with sulfide precipitation as metal removal processes from acid mine drainage in a constructed wetland, *J. Contam. Hydrol.*, 1992, **9**, 115.
3 S. Cole, The emergence of treatment wetlands, *Environ. Sci. Technol.*, 1998, **32**, 218A.
4 S. G. Benner, D. W. Blowes, W. D. Gould, R. B. Herbert, Jr. and C. J. Ptacek, Geochemistry of a permeable reactive barrier for metals and acid mine drainage, *Environ. Sci. Technol.*, 1999, **33**, 2793.
5 R. W. Reisinger and J. Gusek, Mitigation of water contamination at the historic Ferris-Haggerty Mine, Wyoming, *Min. Eng.*, 1999, 49.
6 M. Canty, Innovative *in situ* treatment of acid mine drainage using sulfate-reducing bacteria, in *Proc. Fifth Intl. Conf. on Acid Rock Drainage*, Society for Mining, Metallurgy, and Exploration, Inc (SME), May 2000, pp. 1139–1148.
7 J. J. Gusek, C. Mann, T. R. Wildeman and D. Murphy, Operational results of a 1,200 gpm passive bioreactor for metal mine drainage, West Fork, Missouri, in *Proc. Fifth Intl. Conf. on Acid Rock Drainage*, Society for Mining, Metallurgy, and Exploration, Inc (SME), May 2000, pp. 1133–1138.
8 M. Zaluski, J. Trudnowski, M. Canty and M. A. Harrington-Baker, Performance of field-bioreactors with sulfate-reducing bacteria to control acid mine drainage, in *Proc. Fifth Intl. Conf. on Acid Rock Drainage*, Society for Mining, Metallurgy, and Exploration, Inc (SME), May 2000, pp. 1169–1176.
9 C. H. Gammons, W. Drury and Y. Li, Seasonal influences on heavy metal attenuation in an anaerobic treatment wetlands facility, Butte, Montana, in *Proc. Fifth Intl. Conf. on Acid Rock Drainage*, Society for Mining, Metallurgy, and Exploration, Inc (SME), May 2000, pp. 1159–1168.
10 F. Wang and A. Tessier, Cadmium complexation with bisulfide, *Environ. Sci. Technol.*, 1999, **33**, 4270.
11 D. Dryssen and K. Kremling, Increasing hydrogen sulfide concentration and trace metal behavior in the anoxic Baltic waters, *Mar. Chem.*, 1990, **30**, 193.
12 R. A. Berner, Sedimentary pyrite formation, *Am. J. Sci.*, 1970, **268**, 1.
13 O. Brockamp, E. Goulart, H. Harder and A. Heydemann, Amorphous copper and zinc sulfides in the metalliferous sediments of the Red Sea, *Contrib. Mineral. Petrol.*, 1978, **68**, 85.
14 C. J. Lord and T. M. Church, The geochemistry of saltmarshes: Sedimentary ion diffusion, sulfate reduction, and pyritization, *Geochim. Cosmochim. Acta*, 1983, **47**, 1381.
15 R. J. Davies-Colley, P. O. Nelson and K. J. Williamson, Sulfide control of cadmium and copper concentrations in anaerobic estuarine sediments, *Mar. Chem.*, 1985, **16**, 173.
16 A. T. Herlihy, A. L. Mills and J. S. Herman, Distribution of reduced inorganic sulfur compounds in lake sediments receiving acid mine drainage, *Appl. Geochem.*, 1988, **3**, 333.
17 J. Hamilton-Taylor, W. Davison and K. Morfett, The biogeochemical cycling of Zn, Cu, Fe, Mn, and dissolved organic C in a seasonally anoxic lake, *Limnol. Oceanogr.*, 1996, **41**, 408.
18 J. A. McMahon and W. J. Snodgrass, Chemical equilibrium data bases and tools for calculating zinc sulfide geochemistry in freshwater sediments and its toxicity, *Wat. Qual. Res. J. Can.*, 1996, **31**, 577.
19 M. A. Huerta-Diaz, A. Tessier and R. Carignan, Geochemistry of trace metals associated with reduced sulfur in freshwater sediments, *Appl. Geochem.*, 1998, **13**, 213.
20 R. E. W. Lett and W. K. Fletcher, Syngenetic sulfide minerals in a copper-rich bog, *Miner. Deposita*, 1980, **15**, 61.
21 K. Walton-Day, *Iron and zinc budgets in surface water for a natural wetland affected by acidic mine drainage, St. Kevin Gulch, Lake County, Colorado*, US Geological Survey Water-Resources Investigation Report 94-4014, 1994.
22 A. Sobolewski, *The capacity of natural wetlands to ameliorate water quality: A review of case studies. Proceedings of the Fourth International Conference on Acid Rock Drainage*, Vancouver, Canada, May 31–June 6 1997, pp. 1549–1564.
23 T. R. Wildeman and M. C. Pavlik, Accumulation of metals in a natural wetland that receives acid mine drainage, in *Proc. Fifth International Conference on Acid Rock Drainage*, Society for Mining, Metallurgy, and Exploration, Inc (SME), 2000, pp. 1193–1200.
24 T. E. Duaime, J. J. Metesh, R. N. Bergantino, G. Burns, M. J. Yovich, C. L. Lee-Roark, E. W. Smart and J. F. Ford, Hydrogeologic aspects of remediation of metal mine impacts on Upper Clark Fork Superfund sites, Butte-Warm Springs, Montana, *Northwest Geol.*, 1995, **24**, 99.
25 C. H. Gammons, W. W. Woessner and J. H. Griffin, *Examination of the impacts to the surface-water and groundwater systems of the upper Clark Fork River from 100 years of mining and smelting, in Geologic Field Trips, Western Montana and Adjacent Areas, Rocky Mountain Section of the Geological Society of America*, ed. S. Roberts and D. Winston, The University of Montana and Western Montana College of the University of Montana, Missoula, MT, 2000, pp. 65–84.
26 R. F. Mueller, W. Drury, F. Diebold and W. Chatham, Treatment of metal containing ground and surface water in passive systems, in *Proc. Natl. Meeting of the American Society for Surface Mining and Reclamation*, 1997, p. 15.
27 C. H. Gammons, J. Zhang and P. Wang, Attenuation of heavy metals in a constructed wetlands, Butte, Montana, in *Proc. 1998 Pacific Northwest Regional Meeting of the American Society of Agricultural Engineers: Engineering Biological Processes for Environmental Enhancement*, Paper No. PNW98-129 (ASAE, 29950 Niles Rd., St. Joseph, MI 49085-9659), 1998, p. 9.
28 A. K. Frandsen and C. H. Gammons, Complexation of metals with aqueous sulfide in an anaerobic treatment wetland, in *Proc. Intl. Conf. on Wetlands & Remediation*, Battelle Press, Salt Lake City, 1999, p. 423–430.
29 J. Pantano, R. Bullock, D. McCarthy, T. Sharp and C. Stilwell, Using wetlands to remove metals from mining-impacted groundwater, in *Proc., Intl. Conf. on Wetlands & Remediation*, Battelle Press, Salt Lake City, 1999, pp. 383–390.
30 C. H. Gammons, T. Mulholland and A. K. Frandsen, Comparison of filtered *vs.* unfiltered metal concentrations in aerobic and anaerobic treatment wetlands, *Mine Wat. Environ.*, in the press.
31 A. K. Frandsen, Fate and transport of heavy metals in sulfide-rich waters: applications to anaerobic treatment wetlands, MSc Thesis, Montana Tech of the University of Montana, 2000.
32 S. Jones, Hydraulics of Field-scale Subsurface Flow Constructed Wetlands, MSc Thesis, Montana Tech of the University of Montana, 1997.
33 K. Mainzhausen, Effects of Flow Patterns on Mean Hydraulic Residence Times and on Zinc Removal in Subsurface Flow Constructed Wetlands, MSc Thesis, Montana Tech of the University of Montana, 1998.
34 Ping Wang Chemistry of dissolved, colloidal, and precipitated metals in a constructed wetlands, Butte, Montana, MSc Thesis, Montana Tech of the University of Montana, 1998.
35 Jianming Zhang, Chemical characterization of an upflow organic substrate wetland for treating Butte's Metro Storm Drain water, MSc Thesis, Montana Tech of the University of Montana, 1997.
36 Jianwei Zhang, Removal of metal contamination in water using constructed wetlands: Summary of results from Cells #1, #4, and #6 of the Wetlands Demonstration Project 1, Butte, Montana, MSc Thesis, Montana Tech of the University of Montana, 1998.
37 Pengfei Zhang, Chemical characterization of a horizontal flow organic substrate wetland for treating Butte's Metro Storm Drain water, MSc Thesis, Montana Tech of the University of Montana, 1997.
38 W. Stumm and J. J. Morgan, *Aquat. Chem.*, Wiley, New York, 3rd edn., 1996.
39 R. B. Lorens, Sr, Cd, Mn and Co distribution coefficients in calcite as a function of calcite precipitation rate, *Geochim. Cosmochim. Acta*, 1981, **45**, 553.
40 A. J. Tesoriero and J. F. Pankow, Solid solution partitioning of Sr^{2+}, Ba^{2+}, and Cd^{2+} to calcite, *Geochim. Cosmochim. Acta*, 1995, **60**, 1053.
41 T. S. Lovering, *Organic precipitation of metallic copper*, U. S. Geological Survey Bulletin 795-C, 1927, pp. 45–52.
42 J. D. Forrester, A native copper deposit near Jefferson City, Montana, *Econ. Geol.*, 1942 **37**, 126.
43 J. W. Morse and J. C. Cornwell, Analysis and distribution of iron sulfide minerals in recent anoxic marine sediments, *Mar. Chem.*, 1987, **22**, 55.
44 M. Farrand, Framboidal sulfides precipitated synthetically, *Miner. Deposita*, 1970, **5**, 237.
45 P. B. Barton, Jr. and B. J. Skinner, *Sulfide mineral stabilities in Geochemistry of Hydrothermal Ore Deposits*, ed. H. L. Barnes, Wiley, New York, 2nd edn., 1979, p. 278–403.
46 R. T. Wilkin and H. L. Barnes, Pyrite formation by reactions of iron monosulfides with dissolved inorganic and organic sulfur species, *Geochim. Cosmochim. Acta*, 1996, **60**, 4167.
47 R. T. Wilkin and H. L. Barnes, Formation processes of framboidal pyrite, *Geochim. Cosmochim. Acta*, 1997, **61**, 323.
48 T. Arakaki and J. W. Morse, Coprecipitation and adsorption of Mn(II) with mackinawite (FeS) under conditions similar to those

found in anoxic sediments, *Geochim. Cosmochim. Acta*, 1993, **57**, 9.
49 J. W. Morse and T. Arakaki, Adsorption and co-precipitation of divalent materials with mackinawite (FeS), *Geochim. Cosmochim. Acta*, 1993, **57**, 3635.
50 J. D. Allison, D. S. Brown and K. J. Novo-Gradac, MINTEQA2/PRODEFA2, a geochemical assessment model for environmental systems, US Environmental Protection Agency, EPA/600/3-91/021, 1991.
51 K. D. Daskalakis and G. R. Helz, The solubility of sphalerite (ZnS) in sulfidic solutions at 25 °C and 1 atm pressure, *Geochim. Cosmochim. Acta*, 1993, **57**, 4923.
52 K. Hayashi, A. Sugaki and A. Kitakaze, Solubility of sphalerite in aqueous sulfide solutions at temperatures between 25 and 240 °C, *Geochim. Cosmochim. Acta*, 1990, **54**, 715.
53 A. O. Gubeli and J. Ste. Marie, Constantes de stabilite de thiocomplexes et produits de solubilite de sulfures de metaux. II. Sulfure de zinc, *Can. J. Chem.*, 1967, **45**, 2101.
54 D. Shea and G. R. Helz, The solubility of copper in sulfidic waters: Sulfide and polysulfide complexes in equilibrium with covellite, *Geochim. Cosmochim. Acta*, 1988, **52**, 1815.
55 B. W. Mountain and T. M. Seward, The hydrosulfide/sulfide complexes of copper(I): Experimental determination of stoichiometry and stability at 22 °C and reassessment of high temperature data, *Geochim. Cosmochim. Acta*, 1998, **63**, 11.
56 L. B. Pankratz, A. D. Mah and S. W. Watson, *Thermodyn. Prop. Sulfides*, United States Bureau of Mines, Bull. 689, 1987, p. 427.
57 S. L. Steinberg and H. S. Coonrod, Oxidation of root zone by aquatic plants growing in gravel-nutrient solution culture, *J. Environ. Qual.*, 1984, **23**, 907.
58 D. Shea and G. R. Helz, Solubility product constants of covellite and a poorly crystalline copper sulfide precipitate at 298 K, *Geochim. Cosmochim. Acta*, 1989, **53**, 229.
59 R. A. Thompson and G. R. Helz, Copper speciation in sulfidic solutions at low sulfur activity: Further evidence for cluster complexes?, *Geochim. Cosmochim. Acta*, 1994, **58**, 2971.
60 L. M. Horzempa and G. R. Helz, Controls on the stability of sulfide sols: colloidal covellite as an example, *Geochim. Cosmochim. Acta*, 1979, **43**, 1645.
61 E. J. Silvester, F. Grieser, B. A. Sexton and T. W. Healy, Spectroscopic studies on copper sulfide sols, *Langmuir*, 1991, **7**, 2917.
62 J. Ste. Marie, A. E. Torma and A. O. Gubeli, The stability of thiocomplexes and solubility products of metal sulfides: I. Cadmium sulfide, *Can. J. Chem.*, 1964, **42**, 662.
63 K. D. Daskalakis and G. R. Helz, Solubility of CdS (greenockite) in sulfidic waters at 25 °C, *Environ. Sci. Technol.*, 1992, **26**, 2402.
64 R. A. Berner, Thermodynamic stability of sedimentary iron sulfides, *Am. J. Sci.*, 1967, **265**, 773.
65 W. Davison, N. Philips and B. J. Tabner, Soluble iron sulfide species in natural waters: Reappraisal of their stoichiometry and stability constants, *Aquat. Sci.*, 1999, **61**, 23.
66 J. I. Drever, *The Geochemistry of Natural Waters*, Prentice-Hall, 3rd edn., 1997, Upper Saddle River, New Jersey.
67 G. D. Mironova, A. V. Zotov and N. I. Gul'ko, Determination of the solubility of orpiment in acid solutions at 25–150 °C, *Geochem. Int.*, 1984, **21**, 53.
68 G. D. Mironova, A. V. Zotov and N. I. Gul'ko, The solubility of orpiment in sulfide solutions at 25–150 °C and the stability of arsenic sulfide complexes, *Geochem. Int.*, 1990, **27**, 61.
69 J. G. Webster, The solubility of As_2S_3 and speciation of As in dilute and sulfide-bearing fluids at 25 and 90 °C, *Geochim. Cosmochim. Acta*, 1990, **54**, 1009.
70 L. E. Eary, The solubility of amorphous As_2S_3 from 25 to 90 °C, *Geochim. Cosmochim. Acta*, 1992, **56**, 2267.
71 C. A. Young and R. G. Robins, The solubility of As_2S_3 in relation to the precipitation of arsenic from process solutions, in *Minor Elements 2000: Processing and Environmental Aspects of As, Sb, Se, Te, and Bi*, ed. C. A. Young, Society for Mining, Metallurgy, and Exploration, 2000, in the press.
72 G. R. Helz, J. A. Tossell, J. M. Charnock, R. A. D. Pattrick, D. J. Vaughan and C. D. Garner, Oligomerization in As(III) sulfide solutions: Theoretical constraints and spectroscopic evidence, *Geochim. Cosmochim. Acta*, 1995, **59**, 4591.
73 Montana Department of Environmental Quality, Montana Numeric Water Quality Standards, Circular WQB-7, 1999, p. 35.
74 D. R. Lovley and M. J. Klug, Model for the distribution of sulfate reduction and methanogenesis in freshwater sediments, *Geochim. Cosmochim. Acta*, 1986, **50**, 11.
75 D. A. Sverjensky, E. L. Shock and H. C. Helgeson, Prediction of the thermodynamic properties of aqueous metal complexes to 1000 °C and 5kb, *Geochim. Cosmochim. Acta*, 1997, **61**, 1359.
76 G. W. Luther III, S. M. Theberge and D. T. Rickard, Evidence for aqueous clusters as intermediates during zinc sulfide formation, *Geochim. Cosmochim. Acta*, 1999, **63**, 3169.
77 T. F. Rozan, M. E. Lassman, D. P. Ridge and G. W. Luther III, Evidence for iron, copper and zinc complexation as multinuclear sulfide clusters in oxic rivers, *Nature*, 2000, **406**, 879.
78 C. F. Baes, Jr. and R. E. Mesmer, *The Hydrolysis of Cations*, Wiley, New York, 1976.
79 H. L. Ehrlich, *Geomicrobiology*, Marcel Dekker, New York, 3rd edn., 1996, p. 515.